



**HAL**  
open science

# Towards the time-optimal control of dissipative spin-1/2 particles in nuclear magnetic resonance

M Lapert, Yumeng Zhang, S J Glaser, Dominique Sugny

► **To cite this version:**

M Lapert, Yumeng Zhang, S J Glaser, Dominique Sugny. Towards the time-optimal control of dissipative spin-1/2 particles in nuclear magnetic resonance. *Journal of Physics B: Atomic, Molecular and Optical Physics*, 2011, 44 (15), pp.154014. 10.1088/0953-4075/44/15/154014 . hal-00642391

**HAL Id: hal-00642391**

**<https://hal.science/hal-00642391>**

Submitted on 18 Nov 2011

**HAL** is a multi-disciplinary open access archive for the deposit and dissemination of scientific research documents, whether they are published or not. The documents may come from teaching and research institutions in France or abroad, or from public or private research centers.

L'archive ouverte pluridisciplinaire **HAL**, est destinée au dépôt et à la diffusion de documents scientifiques de niveau recherche, publiés ou non, émanant des établissements d'enseignement et de recherche français ou étrangers, des laboratoires publics ou privés.

# Towards the time-optimal control of dissipative spin 1/2 particles in Nuclear Magnetic Resonance

M. Lapert<sup>1</sup>, Y. Zhang<sup>2</sup>, S. J. Glaser<sup>2</sup> and D. Sugny<sup>1</sup>

<sup>1</sup> Laboratoire Interdisciplinaire Carnot de Bourgogne (ICB), UMR 5209  
CNRS-Université de Bourgogne, 9 Av. A. Savary, BP 47 870, F-21078 DIJON Cedex,  
FRANCE

<sup>2</sup>Department of Chemistry, Technische Universität München, Lichtenbergstrasse 4,  
D-85747 Garching, Germany

E-mail: dominique.sugny@u-bourgogne.fr

**Abstract.** We consider the time-optimal control of a spin 1/2 particle whose dynamics is governed by the Bloch equations with both longitudinal and transverse relaxation terms. We solve this control problem by using geometric optimal control techniques. We show the crucial role of singular extremals in the time-optimal synthesis. This role can mainly be attributed to the presence of dissipation. We also analyze the robustness of the optimal control sequence when both the maximum amplitude of the control field and the dissipative parameters are varied. Finally, we present an experimental implementation of the different solutions using techniques of Nuclear Magnetic Resonance.

PACS numbers: 32.80.Qk,03.65.Yz,78.20.Bh

Submitted to: *J. Phys. B: At. Mol. Phys.*

## 1. Introduction

Nuclear Magnetic Resonance (NMR) is one of the most promising fields of applications of quantum control [1, 2, 3]. In this domain, optimal control techniques can be used to design magnetic fields to control the dynamics of spin systems with applications extending from quantum computing to spectroscopy [4, 5]. In this framework, numerical optimization procedures such as the GRAPE algorithm (Gradient Ascent Pulse Engineering Algorithm) have been developed [6, 7, 8]. Recently, methods of geometric optimal control theory have also been applied with success [9, 10, 11, 12, 13]. This approach which is based on strong mathematical tools coming from differential geometry and Hamiltonian dynamics has a rapid development permitting to attack problems of increasing difficulty [14, 15, 16]. In this context, we have derived in Refs. [17, 18] the complete solution of the optimal control of two-level dissipative quantum systems whose dynamics is governed by the Lindblad equation [19, 20]. We have applied this analysis in Ref. [10] to the time-optimal control of a spin 1/2 particle in a dissipative environment. We have recently extended this work to the energy minimization control problem of a spin [22] and to the control of a spin in presence of both relaxation and radiation damping effects [23]. It is these different results that we propose to review in this paper. In particular, we will show the essential role of singular extremals in the optimal control law. Note that the existence of such singular solutions has been essentially ignored so far in the quantum control literature, and only few results exist [12, 21]. Some parts of the material of this work overlap with Refs. [10, 22, 23], although the presentation is different. We will extend some of these results by constructing the optimal synthesis (i.e. the set of all the optimal solutions starting from the same initial point and reaching any point of the accessible set) and by analyzing the robustness properties of the optimal sequence with respect to variations of the amplitude of the control and of the dissipative parameters. Finally, we refer the reader to the works [17] for a more detailed background on geometric control and proofs of the results.

In this article, we consider the control of a spin 1/2 particle whose dynamics is governed by the Bloch equations with both longitudinal and transverse relaxation terms. As an example, we analyze the saturation problem in minimum time which consists in bringing the magnetization vector from the north pole of the Bloch sphere to the center of the Bloch ball. By its simplicity, this problem can be viewed as a standard textbook problem in quantum control. It is also one of the simplest but non trivial system where all the powerful machinery of geometric control techniques can be applied. The resolution of this control problem will be used to explain some basic tools of geometric optimal control theory. This will help the reader to enter into more specialized mathematical books of optimal control [14, 15, 16].

The paper is organized as follows. We introduce in Sec. 2 the model system used in the computation. Section 3 focuses on the Pontryagin Maximum Principle (PMP) [14, 15, 16] which is the main tool used to solve the control problem. We present some geometric techniques to construct the optimal solution. To simplify the discussion, we

only consider the control of a spin 1/2 particle by one control field. The geometric optimal solutions for the saturation problem are presented in Sec. 4. Both the bounded and the unbounded cases are analyzed. An example of experimental implementation using techniques of Nuclear Magnetic Resonance (NMR) is proposed in Sec. 5. A conclusion and prospective views are given in a final section.

## 2. The model system

We consider a homogeneous ensemble of uncoupled spins 1/2 which are irradiated on resonance by a magnetic field. Homogeneous means here that the resonance offset (or detuning) of each spin is the same. In the rotating frame, the equation of motion can be written as follows [5]:

$$\begin{pmatrix} \dot{M}_x \\ \dot{M}_y \\ \dot{M}_z \end{pmatrix} = \begin{pmatrix} -M_x/T_2 \\ -M_y/T_2 \\ (M_0 - M_z)/T_1 \end{pmatrix} + \begin{pmatrix} \omega_y M_z \\ -\omega_x M_z \\ \omega_x M_y - \omega_y M_x \end{pmatrix}, \quad (1)$$

where the vector of components  $(M_x, M_y, M_z)$  is the magnetization vector and  $M_0$  the equilibrium point of the dynamics along the  $z$ -axis. The dynamics depends on two different terms: A drift term due to the longitudinal and transversal relaxation rates  $T_1^{-1}$  and  $T_2^{-1}$  and a second term representing the effect of the control amplitudes  $\omega_x$  and  $\omega_y$ . We assume that the control field  $\vec{\omega} = (\omega_x, \omega_y, 0)$  satisfies the constraint  $|\vec{\omega}| \leq \omega_{max}$ . We introduce the normalized coordinates  $\vec{x} = (x, y, z) = \vec{M}/M_0$ , which implies that at thermal equilibrium the  $z$  component of the scaled vector  $\vec{x}$  is by definition +1. The normalized control field which satisfies  $|u| \leq 2\pi$  is defined as  $u = (u_x, u_y, 0) = 2\pi\vec{\omega}/\omega_{max}$ , while the normalized time  $\tau$  is given by  $\tau = (\omega_{max}/2\pi)t$ . Dividing the previous system by  $\omega_{max}M_0/(2\pi)$ , one deduces that the dynamics of the normalized coordinates is ruled by the following system of differential equations:

$$\begin{pmatrix} \dot{x} \\ \dot{y} \\ \dot{z} \end{pmatrix} = \begin{pmatrix} -\Gamma x \\ -\Gamma y \\ \gamma - \gamma z \end{pmatrix} + \begin{pmatrix} u_y z \\ -u_x z \\ u_x y - u_y x \end{pmatrix},$$

where  $\Gamma = 2\pi/(\omega_{max}T_2)$  and  $\gamma = 2\pi/(\omega_{max}T_1)$ .

We analyze a control problem where the initial point of the dynamics is the equilibrium point, i.e. the north pole of the Bloch sphere. The goal of the control will be to reach any point of the corresponding accessible set and in particular the center of the Bloch ball. In the setting of NMR spectroscopy and imaging, this latter question corresponds to saturating the signal, e.g., for solvent suppression or contrast enhancement, respectively [24, 25]. Since the initial point is on the  $z$ -axis, the control problem admits a symmetry of revolution around this axis. Without loss of generality, it can be shown that one of the components of the control field can be taken to zero, e.g. here  $\omega_y$  [17]. In the reduced coordinates, this leads to  $u_y = 0$ . We are thus considering

a single input problem in a plane of the form:

$$\begin{pmatrix} \dot{y} \\ \dot{z} \end{pmatrix} = \begin{pmatrix} -\Gamma y \\ \gamma - \gamma z \end{pmatrix} + u \begin{pmatrix} -z \\ y \end{pmatrix},$$

where the subscript  $x$  has been omitted for the control parameter.

This differential system can be written in a more compact form as follows:

$$\dot{\vec{X}} = \vec{F}(\vec{X}) + u\vec{G}(\vec{X}), \quad (2)$$

where the coordinates of the state  $\vec{X}$  of the system are  $(y, z)$  and  $\vec{F}$  and  $\vec{G}$  are two vector fields of components  $(-\Gamma y, \gamma - \gamma z)$  and  $(-z, y)$ .

### 3. The Pontryagin Maximum Principle

We use the PMP to solve the optimal control problem with the constraint of minimizing the control duration [16]. In addition, the field has to satisfy the relation  $|u| \leq 2\pi$ . The PMP is formulated from the pseudo-Hamiltonian  $\mathcal{H}$  which is given in our case by:

$$\mathcal{H} = \vec{P} \cdot (\vec{F}(\vec{X}) + u\vec{G}(\vec{X})), \quad (3)$$

where we have introduced the adjoint state  $\vec{P}$  of components  $(p_y, p_z)$ . The PMP tells us that the optimal solutions are a subset of the set of extremals which are Hamiltonian trajectories of  $\mathcal{H}$  with

$$\dot{\vec{X}} = \frac{\partial \mathcal{H}}{\partial \vec{P}}, \quad \dot{\vec{P}} = -\frac{\partial \mathcal{H}}{\partial \vec{X}}. \quad (4)$$

The optimal control law is given by the maximization condition

$$H(\vec{X}, \vec{P}, v) = \max_{|u| \leq 2\pi} \mathcal{H}(\vec{X}, \vec{P}, u), \quad (5)$$

where  $v$  is the control field maximizing  $\mathcal{H}$  and  $\vec{P}$  a nonzero vector. In addition, since the Hamiltonian  $H$  does not depend on time, one deduces that it is a constant of the motion which is positive by construction of a *maximum principle*,  $H$  being negative in the time-maximum case and zero in the abnormal one [16]. The Hamiltonian equations can be explicitly written in the case of Eq. (2) as  $\dot{\vec{X}} = \vec{F}(\vec{X}) + u\vec{G}(\vec{X})$  and

$$\dot{\vec{P}} = -\vec{P} \cdot \left( \frac{\partial \vec{F}}{\partial \vec{X}} + u \frac{\partial \vec{G}}{\partial \vec{X}} \right), \quad (6)$$

where  $\partial/\partial \vec{X}$  denotes the gradient.  $\partial \vec{F}/\partial \vec{X}$  is a  $2 \times 2$ - matrix whose element of the  $i$ -line and  $j$ -column is equal to  $\partial F_i/\partial X_j$ .

The construction of the optimal solution requires the introduction of two set of points, the singular and the collinear sets which are respectively denoted by  $S$  and  $C$ . The set  $C$  is defined by the points  $\vec{X}$  where the two vectors  $\vec{F}$  and  $\vec{G}$  are collinear. This condition is satisfied if the determinant denoted by  $\det(\cdot, \cdot)$  of the two vectors is zero. We recall that

$$\det(\vec{F}, \vec{G}) = F_1 G_2 - G_1 F_2, \quad (7)$$

where the  $F_i$  and the  $G_i$  are the components of  $\vec{F}$  and  $\vec{G}$ . Here this leads to  $-\Gamma y^2 + \gamma(z - z^2) = 0$ . The set  $C$  is therefore the union of two parabolas if  $\gamma, \Gamma \neq 0$ . The definition of the set  $S$  is more involved since it is given by the relation  $\det(\vec{G}, [\vec{F}, \vec{G}]) = 0$ ,  $[\vec{F}, \vec{G}]$  being the commutator of two vector fields which can be computed as follows in the coordinates  $x_i$ :

$$[\vec{F}, \vec{G}]_j = \sum_i \left( \frac{\partial G_j}{\partial x_i} F_i - \frac{\partial F_j}{\partial x_i} G_i \right).$$

In our example, one arrives at

$$2\Gamma yz + \gamma(y - 2yz) = 0.$$

One deduces that  $S$  corresponds to the union of the vertical line  $y = 0$  and of the horizontal one  $z = z_0$  given by

$$z_0 = -\frac{\gamma}{2(\Gamma - \gamma)} = -\frac{T_2}{2(T_1 - T_2)}$$

if  $\Gamma \neq \gamma$  (or equivalently if  $T_1 \neq T_2$ ). In the case  $\Gamma \leq \frac{3}{2}\gamma$  then only the vertical line exists. The two sets  $S$  and  $C$  are displayed in Fig. 1 for a given set of parameters.

Returning back to the PMP, one sees that the maximization condition can be solved by introducing the switching function  $\Phi = \vec{P} \cdot \vec{G} = -p_y z + p_z y$  [16]. Using Eq. (5) and the fact that the drift term  $\vec{P} \cdot \vec{F}$  of  $\mathcal{H}$  cannot be controlled, one immediately deduces that the control field  $u$  is given by

$$u = 2\pi \times \text{sign}[\Phi(t)]$$

if  $\Phi(t) \neq 0$ . Such a point is said to be regular. The corresponding control of constant amplitude is called bang. A time such that the control changes sign is a switching time. Such a case occurs when  $\Phi$  vanishes in an isolated point  $t = t_0$ . This is associated to a bang-bang control sequence. The singular situation corresponds to the case where  $\Phi$  is equal to zero on an interval  $[t_0, t_1]$ . At this point, a crucial remark is the fact that the singular trajectories lie in the set  $S$ . This can be shown by using the relation  $\Phi(t) = \dot{\Phi}(t) = 0$  on the interval  $[t_0, t_1]$ . The first derivative of  $\Phi$  can be determined as follows. We have:

$$\dot{\Phi} = \dot{\vec{P}} \cdot \vec{G} + \vec{P} \cdot \dot{\vec{G}}.$$

Using Eq. (4) and  $\dot{\vec{G}} = \frac{\partial \vec{G}}{\partial \vec{X}} \cdot \dot{\vec{X}}$ , one gets that:

$$\dot{\Phi} = \vec{P} \cdot [\vec{F}, \vec{G}].$$

The system  $\Phi(t) = \dot{\Phi}(t) = 0$  admits a non zero  $\vec{P}$  solution if the vectors  $[\vec{F}, \vec{G}]$  and  $\vec{G}$  are parallel, i.e. if  $\det(\vec{G}, [\vec{F}, \vec{G}]) = 0$ . This first computation does not give the explicit form of the singular control  $u_s$ , which is obtained from the second derivative of  $\Phi$ . Indeed, a similar computation to the one for  $\dot{\Phi}$  leads to:

$$\ddot{\Phi} = \vec{P} \cdot [[\vec{G}, \vec{F}], \vec{F}] + u \vec{P} \cdot [[\vec{G}, \vec{F}], \vec{G}],$$

and we get that

$$u_s = -\frac{\vec{P} \cdot [[\vec{G}, \vec{F}], \vec{F}]}{\vec{P} \cdot [[\vec{G}, \vec{F}], \vec{G}]}$$

if  $\vec{P} \cdot [[\vec{G}, \vec{F}], \vec{G}] \neq 0$ . If this latter relation is not satisfied, derivatives of higher orders have to be computed to determine  $u_s$ .

In our case, one arrives at:

$$u_s(y, z) = \frac{-y\gamma(\Gamma - 2\gamma) - 2yz(\gamma^2 - \Gamma^2)}{2(\Gamma - \gamma)(y^2 - z^2) - \gamma z}, \quad (8)$$

which simplifies into  $u_s = 0$  for the vertical singular line and into

$$u_s = \frac{\gamma(\gamma - 2\Gamma)}{2(\Gamma - \gamma)y}$$

for the horizontal one where  $z = z_0$ . It can also be checked that the denominator is different from zero on the set  $S$ , except at the intersection of the two singular lines. Another important point is the admissibility of the singular control since by definition of the control problem we must have  $|u_s| \leq 2\pi$ . Using Eq. (8), one deduces that the singular control is admissible on the horizontal line if  $|y| \geq |\gamma(\gamma - 2\Gamma)|/[2\pi(2\Gamma - 2\gamma)]$ . For smaller values of  $y$ , the system cannot follow the horizontal singular arc and must leave this line by using a bang pulse. A consequence of this phenomenon, which is called a saturation of the control field, is the creation of a switching curve starting from the point where the field loses its admissibility [16]. A switching line is a line such that the optimal control changes sign when crossing it. This curve can be constructed numerically as explained in Sec. 4.

From this first analysis, we know that the extremal trajectories will be the concatenation of bang arcs of maximum or minimum amplitude and of singular arcs on the set  $S$ . However, this study tells us nothing about the optimality status of the extremals. This optimality can be in some cases determined from the clock form.

#### The clock form

We derive in this paragraph the expression of the clock form denoted  $\alpha$  [15]. By definition, the clock form is a 1-form, i.e. a linear functional on the space of vector fields, which fulfills the following conditions

$$\begin{cases} \alpha(\vec{F}) = 1 \\ \alpha(\vec{G}) = 0 \end{cases} .$$

A solution of this system exists except on the set  $C$  where  $\vec{F}$  and  $\vec{G}$  are collinear. Indeed, assuming that  $\vec{F} = \beta\vec{G}$  where  $\beta$  is a scalar function, one then deduces that

$$1 = \alpha(\vec{F}) = \beta\alpha(\vec{G}) = 0$$

which gives a contradiction. We write  $\alpha$  as  $\alpha = \alpha_y dy + \alpha_z dz$  where  $dy$  and  $dz$  are the differentials of the coordinates  $y$  and  $z$ . We recall that  $dy$  is a mapping which associates

to any vector field its  $y$ - coordinate. Simple algebra shows that  $\alpha_y$  and  $\alpha_z$  are solutions of the system

$$\begin{cases} \alpha_y(-\Gamma y) + \alpha_z(\gamma - \gamma z) = 1 \\ \alpha_y z = \alpha_z y \end{cases}.$$

We obtain that

$$\begin{cases} \alpha_y = \frac{-y}{\Gamma y^2 - \gamma z + \gamma z^2} \\ \alpha_z = \frac{-z}{\Gamma y^2 - \gamma z + \gamma z^2} \end{cases}.$$

From the 1-form  $\alpha$ , we can define the 2-form  $d\alpha$  which is given by

$$d\alpha = \left( \frac{\partial \alpha_z}{\partial y} - \frac{\partial \alpha_y}{\partial z} \right) dy \wedge dz,$$

and reads after some calculations

$$d\alpha = \frac{2\Gamma yz + \gamma y - 2\gamma yz}{[\Gamma y^2 - \gamma z + \gamma z^2]^2} dy \wedge dz.$$

If we write  $d\alpha$  as  $d\alpha = g(y, z)dy \wedge dz$  then one sees that  $g(y, z) = 0$  on  $S$  and that  $g$  is infinite on  $C$ . It is then straightforward to deduce that the function  $g$  has a constant sign in the regions delimited by the lines of  $S$ . This point is represented on Fig. 1 for a given set of parameters. Four quadrants with different signs of  $g$  are displayed. As

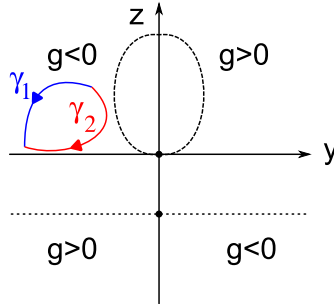


**Figure 1.** (Color Online) Sign of the function  $g$  in the plane  $(y, z)$ . The dashed and dotted lines indicate respectively the positions of the collinear locus and the horizontal singular line (see the text). Two paths  $\gamma_1$  and  $\gamma_2$  are plotted in blue (dark) and red (dark gray) to illustrate the use of the clock form.

suggested by its name, the clock form is a form which allows one to determine the time taken to travel a path and to compare the extremals. Let  $\gamma$  be a path in the plane  $(y, z)$  which does not cross  $C$  and  $T$  the time of travel along  $\gamma$ . We have

$$\int_{\gamma} \alpha = \int_0^T \alpha(\dot{X}) dt = \int_0^T \alpha(\vec{F}) dt = T.$$

We consider now two paths  $\gamma_1$  and  $\gamma_2$  starting and ending at the same points and respectively associated to the durations  $T_1$  and  $T_2$  (see Fig. 1 for an illustrative example). One shows by using the Stokes theorem that

$$T_1 - T_2 = \int_{\gamma_1} \alpha - \int_{\gamma_2} \alpha = \int_D d\alpha,$$

where  $D$  is the surface delimited by  $\gamma_1 \cup -\gamma_2$ . For paths  $\gamma_1$  and  $\gamma_2$  which lie in one of the four quadrants defined by  $S$ , we can straightforwardly determine the time-optimal trajectory. For instance on the Fig. 1, the time to travel the path  $\gamma_1$  is lower than the one to travel  $\gamma_2$  since the two paths belong to a region with  $g < 0$ .

Using such arguments, we can also analyze the optimality of singular lines. The proof uses a singular path and a path starting and ending on the singular line but associated to a bang-bang control. Note that this result is only a local optimality result in the sense that the singular trajectory is optimal for any neighboring initial and final points on this axis. The difference between local and global optimality will be detailed in Sec. 4. In the example of Sec. 4, it can be shown that the horizontal singular line is optimal and that the vertical one is optimal only if  $z > z_0$ .

#### 4. Time-optimal control of spin 1/2 particles

We apply in this section the tools of Sec. 3 to the control of spin 1/2 particles. We begin our study by considering the control problems defined by the relaxation parameters  $\gamma^{-1}$  and  $\Gamma^{-1}$  (expressed in the normalized time unit defined above) of 23.9 and 1.94, respectively and  $M_0 \approx 2.15 \times 10^{-5}$ . Such values of the parameters correspond to a realistic experimental situation in NMR where  $T_1 = 740$  ms,  $T_2 = 60$  ms and  $\omega_{max}/(2\pi) = 32.3$  Hz [10].

##### 4.1. Optimal synthesis

This paragraph is rather technical and describes the way to construct the optimal synthesis, which is the set of all the optimal sequences starting from the north pole of the dynamics and reaching any point of the corresponding accessible set  $\mathcal{A}$ . Since the control field cannot fully compensate the effect of dissipation [26, 27], the system is not controllable and all the points of the Bloch ball cannot be reached. In this case, the reachable set can be determined by the explicit construction of all the trajectories satisfying the constraint  $|u| \leq 2\pi$  (see Fig. 2 for an example). More precisely, we first search for the boundary of this set, i.e. the trajectories with  $u = \pm 2\pi$  originating from the north pole. Then we show that all the points inside the boundary are attainable by the explicit construction of the optimal control laws as displayed in Fig. 2.

The application of the PMP gives only the local behavior of the extremals. In particular, we know that the optimal solutions are the concatenations of bang arcs of amplitude  $\pm 2\pi$  and of singular optimal arcs. Different extremal solutions which are locally optimal can be used to reach the same target state. The last step of the optimal synthesis consists of choosing among these extremals the time-minimizing one, which corresponds to the optimal one. This choice can be done by using the clock form and numerical comparisons of extremals when the paths cross the singular or the collinear loci. Note also that neighboring optimal trajectories have the same structure, except in presence of particular lines, i.e. the switching curve and lines belonging to the sets  $S$

and  $C$ .

The corresponding optimal synthesis is represented in Fig. 2. In the numerical examples, the switching curve has been determined numerically by considering a series of trajectories with  $u = +2\pi$  originating from the horizontal singular set where  $\Phi = 0$ . The points of the switching curve correspond to the first point of each trajectory where the switching function vanishes. In Fig. 2, we observe that the optimal trajectory can have different structures extending from bang-bang arcs to bang-singular-bang-bang and bang-singular-bang-singular arcs. A bang-singular-bang-bang control is, e.g., the concatenation of a bang-bang arc followed by a singular and a bang arc.

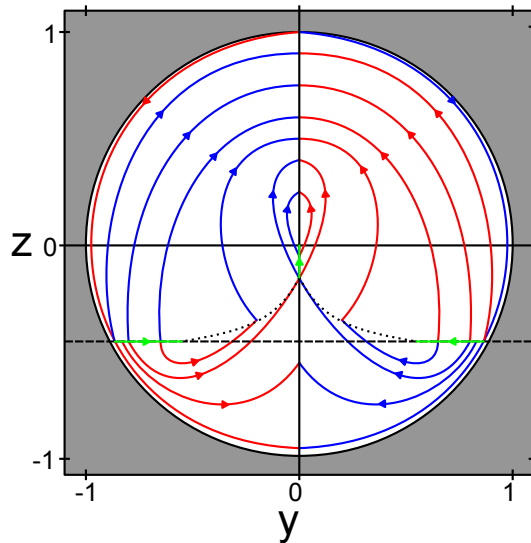


**Figure 2.** (Color Online) Schematic representation of the optimal synthesis when the initial point of the dynamics is the north pole. An arbitrary zoom has been used to construct the figure. Regular curves are plotted in blue (dark) and red (dark gray) for control fields equal to  $+2\pi$  and  $-2\pi$ , respectively. The optimal singular trajectories are displayed in green (light gray). The dotted line is the switching curve, while the dashed one is the non-admissible part of the horizontal singular line. The small arrows indicate the way the curves are traveled.

#### 4.2. The saturation control problem

In this paragraph, we analyze the saturation control problem which consists in bringing the initial state vector to the center of the Bloch ball in minimum time. We compare the optimal control law with an intuitive one used in NMR, the inversion recovery sequence [24, 25]. The intuitive solution is composed of a bang pulse to reach the opposite point of the initial state along the  $z$ -axis followed by a zero control where we let the dissipation act up to the center of the Bloch ball. The optimal and the intuitive solutions are plotted in Fig. 3. Using results of the previous section, one deduces that the optimal control is the concatenation of a bang pulse, followed successively by a singular control along the horizontal singular line, another bang pulse and a zero singular control along

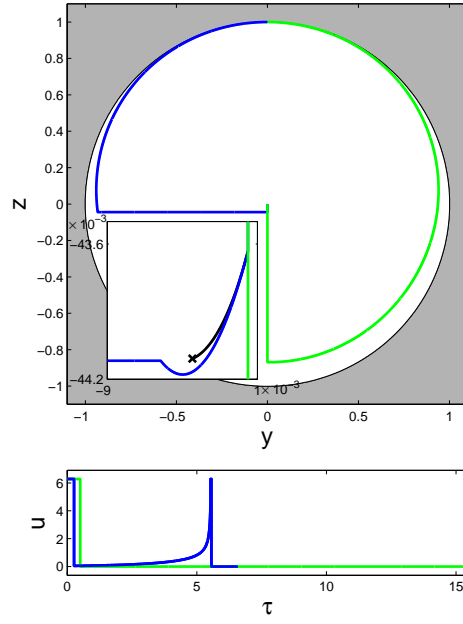


**Figure 3.** (Color online) Plot of the optimal trajectories (blue or dark gray) and of the Inversion Recovery sequence (green of light gray) in the plane  $(y, z)$ . The corresponding control laws are represented in the lower panel. In the upper panel, the small insert represents a zoom of the optimal trajectory near the origin. The black line is the switching curve originating from the horizontal singular line. The cross indicates the position of the admissibility point. The vertical line corresponds to the intuitive solution. The blue (or dark gray) curve is the optimal trajectory near the origin.

the vertical singular line. The dynamics leaves the horizontal line before the limit of admissibility at a point of coordinates  $(y_0, z_0)$ . The coordinate  $y_0$  can be determined numerically as follows. We consider the bang arc starting from  $(y_0, z_0)$  and we compute  $\Phi$  and  $\dot{\Phi}$  along this trajectory.  $y_0$  is then characterized by the fact that  $\Phi = \dot{\Phi} = 0$  at the intersection point of the extremal with the vertical singular line. Figure 3 displays also the switching curve. We have checked that the second bang pulse of the optimal sequence does not cross the switching curve up to the vertical singular axis. In this example, the center of the Bloch ball is reached with an accuracy better than  $10^{-15}$ . The durations of the two sequences are 202 ms for the optimal solution and 478 ms for the IR one. One therefore sees that a gain of 58% is obtained for the optimal solution over the intuitive one.

This result also highlights the role of singular extremals. The two solutions considered use singular controls, along the horizontal and the vertical lines for the optimal sequence and along the vertical axis for the IR solution. The difference between the two trajectories comes from the fact that the singular controls are optimal for the optimal law, while it is not the case for the IR one.

The ratio between the two control durations can be analytically computed in the

unbounded case where there is no bound on the control. More precisely, this means that we consider the limit  $\omega_{max} \rightarrow +\infty$ . In this case, the optimal solution is only composed of a bang arc followed by singular controls along the horizontal and the vertical lines since there is no admissibility condition on the control (see also the discussion of Sec. 4.3). We first compute the duration of the IR sequence. In the limit of an infinite bound on the control, the first bang allows to reach instantaneously the south pole of the Bloch sphere. The second part of the control uses the longitudinal dissipation with a zero control field to go to the center of the sphere. The dynamics is governed by:

$$\dot{z} = \frac{1}{T_1}(1 - z). \quad (9)$$

In this computation, note that the parameters  $\Gamma$  and  $\gamma$  and the reduced time  $\tau$  cannot be used since they depend on the bound  $\omega_{max}$ . The solution of Eq. (9) is  $z(t) = (z(0) - 1)e^{-\frac{t}{T_1}} + 1$  with  $z(0) = -1$ . We next determine the time  $t_1$  such that  $z(t_1) = 0$ . Inverting this equation, we find the time  $t_1 = T_1 \ln(1 - z(0)) = T_1 \ln 2$ . For the optimal solution, the first step is to use a bang pulse to reach instantaneously the horizontal singular line in a point of coordinates  $(y, z_0)$  (with  $z_0 = \frac{T_2}{2(T_2 - T_1)}$  and  $y^2 + z_0^2 = 1$ ). The second step consists of following this line. We know that the dynamics and the singular control satisfy:

$$\begin{cases} \dot{y} = -\frac{1}{T_2}y - u_s z_0 \\ u_s = -\frac{1}{2T_1} \frac{2T_1 - T_2}{T_1 - T_2} \frac{1}{y} \end{cases}. \quad (10)$$

The dynamics reduces to:

$$\dot{y} = -\frac{1}{T_2}y - \frac{2T_1 - T_2}{4(T_1 - T_2)^2} \frac{T_2}{T_1} \frac{1}{y}, \quad (11)$$

and if we consider the change of variable  $Y = y^2$ , we get:

$$\dot{Y} = -2Y/T_2 - \alpha, \quad (12)$$

where  $\alpha = \frac{2T_1 - T_2}{4(T_1 - T_2)^2} \frac{T_2}{T_1}$ . The solution of this equation is

$$Y(t) = \left(\frac{\alpha T_2}{2} + Y(0)\right)e^{-2\frac{t}{T_2}} - \frac{\alpha T_2}{2}.$$

Starting from the coordinate  $Y(0) = 1 - z_0^2$  and following the singular line up to  $Y(t) = 0$ , we find the duration  $t_2 = \frac{T_2}{2} \ln\left(1 + \frac{2Y(0)}{\alpha T_2}\right)$ . The last part of the optimal solution uses the vertical singular line with  $u = 0$ . The same expression as for the I.R. solution leads with  $z(0) = z_0$  to  $t_3 = T_1 \ln(1 - z_0)$ . Finally, one arrives at:

$$\begin{cases} T_{opt} = \frac{T_2}{2} \ln\left(1 + \frac{2(1 - z_0^2)}{\alpha T_2}\right) + T_1 \ln(1 - z_0) \\ T_{IR} = T_1 \ln 2 \end{cases} \quad (13)$$

where  $T_{opt} = t_2 + t_3$  and  $T_{IR} = t_1$ . As can be expected, the two times only depend on the two relaxation parameters  $T_1$  and  $T_2$ . The optimal solution uses actively the transverse relaxation to reach in minimum time the target state. In our example, the ratio of the two durations is equal to 0.383. A complete numerical study shows that this ratio decreases as  $\omega_{max}$  increases and tends asymptotically towards the value of the unbounded case [10].

### 4.3. Robustness of the optimal solution

We analyze in this section the robustness of the structure of the optimal solution with respect to variations of dissipative parameters and of the bound on the control.

We first consider that the bound of the control field is varied. In this paragraph, we assume that the control field satisfies  $|u| \leq 2\pi \times u_0$  where  $u_0$  can be changed at will and we fix the dissipative parameters. In this case, three different structures can be found as shown in Fig. 5. When  $u_0$  is sufficiently small, the first bang arc does not intersect the horizontal singular line and the optimal solution is the concatenation of a bang arc followed by a vertical singular arc. When  $u_0 \simeq 1$ , we recover the standard situation described in Sec. 4.2 where the system leaves the horizontal singular line just before the limit of admissibility. It can be shown that this situation is generic in the sense that the intersection point of the initial bang arc with the horizontal singular line belongs to the admissible part of this line. The proof goes as follows. We know that the limit of admissibility is defined by:

$$y_0 = \frac{\gamma(\gamma - 2\Gamma)}{4\pi u_0(\Gamma - \gamma)},$$

$$z_0 = -\frac{\gamma}{2(\Gamma - \gamma)}.$$

We then determine the limiting case where the bang arc intersects the singular line. This corresponds to the tangency of the two curves, which is schematically represented in Fig. 4. The tangency occurs when  $\dot{z} = 0$  and  $z = z_0$ , which leads to the relations

$$\gamma(1 - z_0) + 2\pi u_0 y = 0$$

and

$$y = -\frac{\gamma(1 - z_0)}{2\pi u_0} = y_0.$$

We can conclude that the bang arc is tangent to the singular line when their intersection

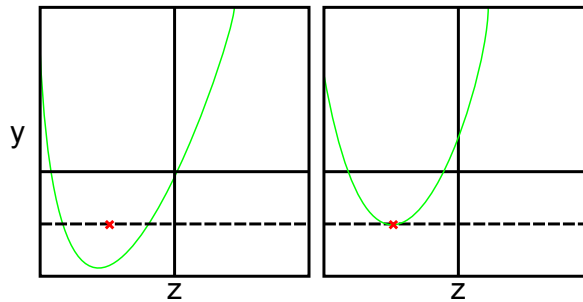


**Figure 4.** (Color Online) Schematic evolution of a bang arc in green (light gray) starting from the equilibrium point of the dynamics when the maximum bound on the control is decreased (from left to right). The horizontal dashed line is the horizontal singular line, while the red (black) cross represents the limit of admissibility.

point is the point of coordinates  $(y_0, z_0)$ .

In the limit  $u_0 \rightarrow +\infty$ , the first bang arc belongs to the Bloch sphere and the limit point of admissibility tends to the vertical axis. This explains the change of structure in the unbounded case where the control is the succession of a bang, a horizontal singular arc and a vertical one.

Figure 6 displays the evolution of the optimal trajectories when the dissipative parameter  $T_2$  varies,  $T_1$  being fixed. Numerical values are taken to be 444, 386, 295, 138 and 60 ms from bottom to top, which correspond in the reduced coordinates to a parameter  $\Gamma$  equal to 0.0697, 0.0803, 0.1048, 0.2241 and 0.5160. If we denote by  $z = a$  the position of the horizontal singular extremal then we have  $T_2 = 2aT_1/(2a - 1)$ . Figure 6 shows that the different extremals present the same qualitative structure with a pulse sequence composed of a bang, a horizontal singular, a bang and a vertical singular extremal to reach the origin. The optimal trajectories only differ in the durations of the bang and singular arcs. Two limiting cases can be considered. The first one corresponds to  $a = 0$ , which can be associated in a practical situation to the relation  $T_2 \ll T_1$  or  $\gamma \ll \Gamma$ , i.e. the longitudinal relaxation is negligible with respect to the transverse one. The optimal solution is then composed of a bang arc followed by a horizontal singular arc with  $z = 0$  up to the center of the Bloch ball. Along this arc, we have  $u_s = 0$  since  $\gamma = 0$ . The other limiting case is  $a = -1$ , i.e.  $T_2 = 2T_1/3$ , for which the IR sequence is the optimal solution. This conclusion is also true for  $a < -1$ .

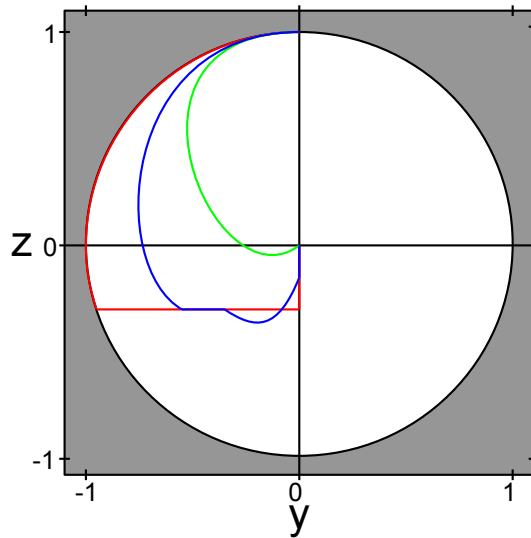


**Figure 5.** (Color Online) Plot of the optimal trajectories for different bounds on the control field. The green (light gray) extremal curve does not intersect the horizontal singular line. The blue (dark) trajectory has the generic structure described in Sec. 3, while the red (dark gray) one corresponds to the unbounded case.

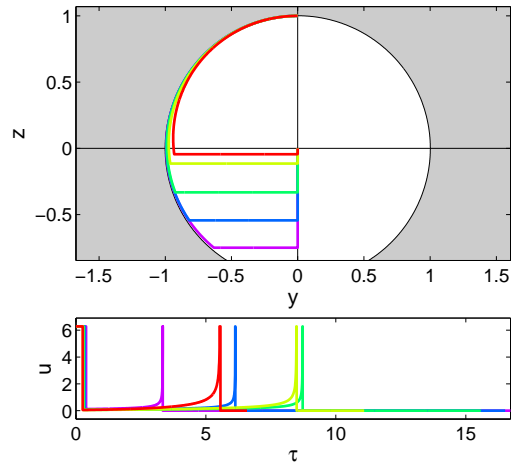


**Figure 6.** (Color Online) (top) Evolution of the magnetization vector along the optimal trajectory for different dissipative parameters (bottom) The corresponding control fields  $u$ .

## 5. Experimental implementation

In this work, we consider NMR control experiments in liquid state. Such experiments present some key advantages with respect to other domains of quantum control such as, e.g., the control of atomic and molecular dynamics by laser fields. They can be summarized as follows. The models used in NMR reproduce with great accuracy the experimental conditions even for very complex molecular structures such as proteins in presence of an interaction with an environment. The typical error between theory and experiment is of the order of few percents. In addition, very complex control fields can be shaped experimentally, which reinforces the interest of theoretical studies. To illustrate these properties, we detail below the case of the saturation control problem. Figure 7 presents some experimental data for the time-optimal saturation control problem. The parameters of Sec. 4 have been used in the experiments which were performed on the  $^1\text{H}$  proton spins of  $\text{H}_2\text{O}$  at room temperature (298 K) in a sample constituted of 10%  $\text{H}_2\text{O}$ , 45%  $\text{D}_2\text{O}$ , and 45% deuterated glycerol saturated with  $\text{CuSO}_4$ . The experiments were done on a Bruker Avance 600 MHz spectrometer with linearized amplifiers. As already mentioned below, we observe in Fig. 7 the very good agreement between theoretical curves and experimental points. This agreement confirms that such kind of optimal trajectories can be implemented with modern NMR spectrometers.

## 6. Conclusion and prospective views

Our goal in the research reported in this paper has been to explore the time-optimal control of a spin 1/2 particle in presence of relaxation effects. Completing previous research

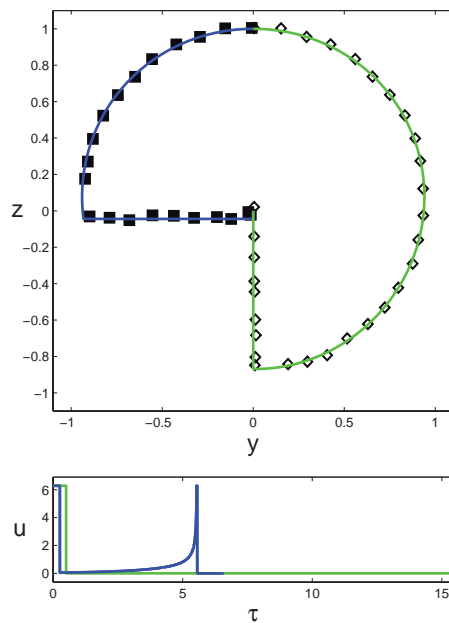


**Figure 7.** (Color Online) Plot of the optimal trajectories (blue or dark gray curve) and of the inversion recovery sequence (green or gray curve) in the plane  $(y, z)$  for  $T_1 = 740$  ms,  $T_2 = 60$  ms and  $\omega_{max}/(2\pi) = 32.3$  Hz. Filled squares and open diamonds correspond to the experimentally measured points. The lower panel displays the control laws.

in this field, this work gives a general overview of the construction and of the determination of the optimal solution, which combines a geometric analysis and analytical and numerical computations. However, it is clear that much remains to be accomplished in the application of geometric optimal techniques to quantum control. Up to now, only very simple quantum systems have been considered. A challenging task in a near future will be to extend such works to more complicated systems. In this perspective, we have applied this method to the optimal control of two uncoupled spin systems in Ref. [11] and we are actually working on the control of three and four spins. Such studies will be interesting from both a fundamental perspective and for possible applications in NMR spectroscopy and imaging in order to take into account experimental constraints such as resonance offsets and control field inhomogeneities. However, some theoretical and numerical limitations may exist. According to the Pontryagin Maximum Principle, the optimal solutions are computed from a shooting equation, by determining the initial adjoint vector, which selects the extremal trajectory reaching the target state. The resolution of this equation is more and more difficult when the complexity of the system increases or when the chaotic behavior of the associated classical dynamic becomes predominant. In this case, a possibility is to use a continuation method when the control problem depends on a parameter (e.g. the relaxation rates). The continuation approach is used to solve step by step the shooting equation, the solution of an initial problem being known. In addition, even in a very complicated situation where purely numerical

algorithms such as the GRAPE one has to be used, the geometric techniques can be interesting. One can find the geometric solution of a simpler problem and then use this control law as a trial solution of the numerical algorithm. This helps the convergence of the algorithm and guides it towards a solution close to the geometric one. We have shown the efficiency of this coupling between the two methods in [23] in order to solve the saturation control problem of a large number of spins with different resonance offsets due to experimental imperfections.

**Acknowledgment** S.J.G. acknowledges support from the DFG (GI 203/6-1), SFB 631, the EU program Q-ESSENCE, and the Fonds der Chemischen Industrie. Experiments were performed at the Bavarian NMR center at TU Munchen.

## References

- [1] Rice S. and Zhao M. 2000 *Optimal control of quantum dynamics*, (Wiley, New-York)
- [2] Shapiro M. and Brumer P. 2003 *Principles of quantum control of molecular processes*, (Wiley, New-York)
- [3] Tannor D. J. 2007 *Introduction to quantum mechanics: A time-dependent perspective*, (University Science Books, Sausalito)
- [4] Ernst R. R. 1990 *Principles of Nuclear Magnetic Resonance in one and two dimensions* (International Series of Monographs on Chemistry, Oxford University Press, Oxford)
- [5] Levitt M. H. 2008 *Spin dynamics: basics of nuclear magnetic resonance* (John Wiley and sons, New York-London-Sydney)
- [6] Khaneja N., Reiss T., Kehlet C., Schulte-Herbrüggen T. and Glaser S. J. 2005 *J. Magn. Reson.* **172**, 296
- [7] Skinner T. E., Reiss T. O., Luy B., Khaneja N. and Glaser S. J. 2003 *J. Magn. Reson.* **163**, 8; Skinner T. E., Reiss T. O., Luy B., Khaneja N. and Glaser S. J. 2004 *J. Magn. Reson.* **167**, 68; Kobzar K., Skinner T. E., Khaneja N., Glaser S. J. and Luy B. 2004 *J. Magn. Reson.* **170**, 236; Skinner T. E., Reiss T. O., Luy B., Khaneja N. and Glaser S. J. 2005 *J. Magn. Reson.* **172**, 17; Skinner T. E., Kobzar K., Luy B., Bendall R., Bermel W., Khaneja N. and Glaser S. J. 2006 *J. Magn. Reson.* **179**, 241; Gershenson N. I., Kobzar K., Luy B., Glaser S. J. and Skinner T. E. 2007 *J. Magn. Reson.* **188**, 330.
- [8] Zhu W., Botina J. and Rabitz H. 1998 *J. Chem. Phys.* **108**, 1953; Maximov I. I., Salomon J., Turinici G. and Nielsen N. C. 2010 *J. Chem. Phys.* **132**, 084107; Sugny D., Kontz C., Ndong M., Justum Y. and Desouter-Lecomte M. 2006 *Phys. Rev. A* **74**, 043419; Sugny D., Ndong M., Lauvergnat D., Justum Y. and Desouter-Lecomte M. 2007 *J. Photochem. Photobiol. A* **190**, 359; Lapert M., Tehini R., Turinici G. and Sugny D. 2008 *Phys. Rev. A* **78**, 023408 (2008); Lapert M., Tehini R., Turinici G. and Sugny D. 2009 *Phys. Rev. A* **79**, 063411
- [9] Khaneja N., Brockett R. and Glaser S. J. 2001 *Phys. Rev. A* **63**, 032308; Khaneja N., Glaser S. J. and Brockett R. 2002 *Phys. Rev. A* **65**, 032301; Yuan H. and Khaneja N. 2005 *Phys. Rev. A* **72**, 040301(R)
- [10] Lapert M., Zhang Y., Braun M., Glaser S. J. and Sugny D. 2010 *Phys. Rev. Lett.* **104**, 083001
- [11] Assémat E., Lapert M., Zhang Y., Braun M., Glaser S. J. and Sugny D. 2010 *Phys. Rev. A* **82**, 013415
- [12] Boscain U. and Mason P. 2006 *J. Math. Phys.* **47**, 062101
- [13] Stefanatos D. 2009 *Phys. Rev. A* **80**, 045401
- [14] Jurdjevic V. 1996 *Geometric control theory* (Cambridge University Press, Cambridge)
- [15] Bonnard B. and Chyba M. 2003 *Singular trajectories and their role in control theory* (Springer SMAI, Vol. 40)

- [16] Boscain U. and Piccoli B. 2004 *Optimal syntheses for control systems on 2-D manifolds* (Mathématiques and Applications, 43, Springer-Verlag, Berlin)
- [17] Sugny D., Kontz C. and Jauslin H. R. 2007 Phys. Rev. A **76**, 023419; Bonnard B. and Sugny D. 2009 SIAM J. on Control and Optimization, **48**, 1289; Bonnard B., Chyba M. and Sugny D. 2009 IEEE Transactions on Automatic control, **54**, 11, 2598; Sugny D. and Kontz C. 2008 Phys. Rev. A **77**, 063420
- [18] Bonnard B., Cots O., Scherbakova N. and Sugny D. 2010 J. Math. Phys. **51**, 092705
- [19] Lindblad G. 1976 Commun. Math. Phys. **48**, 119
- [20] Gorini V., Kossakowski A. and Sudarshan E. C. G. 1976 J. Math. Phys. **17**, 821
- [21] Sklarz S. E., Tannor D. J. and Khaneja N. 2004 Phys. Rev. A **69**, 053408; Tannor D. J. and Bartana A. 1999 J. Phys. Chem. A **103**, 10359
- [22] Lapert M., Zhang Y., Braun M., Glaser S. J. and Sugny D. 2010 Phys. Rev. A **82**, 063418
- [23] Zhang Y., Braun M., Lapert M., Sugny D. and Glaser S. J. 2011 J. Chem. Phys. **134**, 054103
- [24] Bydder G. M., Hajnal J. V. and Young I. R. 1998 Clinical Radiology **53**, 159
- [25] Patt S. L. and Sykes B. D. 1972 J. Chem. Phys. **56**, 3182
- [26] Altafini C. 2003 J. Math. Phys. **44**, 2357
- [27] Altafini C. 2004 Phys. Rev. A **70**, 062321